

Supporting Information

# Hydrogel-Incorporating Unit in a Well: 3D Cell Culture for High-Throughput Analysis

Yeong Jun Yu,<sup>ab</sup> Young Hye Kim,<sup>a</sup> Kyuhwan Na,<sup>c</sup> Seo Yun Min,<sup>a</sup> Ok Kyung Hwang,<sup>de</sup>  
Da Kyeong Park,<sup>a</sup> Doo Yeon Kim,<sup>f</sup> Se Hoon Choi,<sup>f</sup> Roger D. Kamm,<sup>g</sup> Seok Chung,<sup>\*bc</sup> and Jeong  
Ah Kim<sup>\*ah</sup>

<sup>a</sup>*Biomedical Omics Group, Korea Basic Science Institute, Chungbuk 28119, Republic of Korea*

<sup>b</sup>*Program in Micro/Nano System, Korea University, Seoul 02841, Republic of Korea*

<sup>c</sup>*School of Mechanical Engineering, Korea University, Seoul 02841, Republic of Korea*

<sup>d</sup>*New Drug Development Center, Osong Medical Innovation Foundation, Chungbuk 28160, Republic of Korea*

<sup>e</sup>*College of Pharmacy and Medical Research Center, Chungbuk National University, Chungbuk 28160, Republic of Korea*

<sup>f</sup>*Genetics and Aging Research Unit, MassGeneral Institute for Neurodegenerative Disease, Massachusetts General Hospital, Harvard Medical School, Charlestown, MA 02129, USA*

<sup>g</sup>*Department of Mechanical Engineering, Massachusetts Institute of Technology, Cambridge, MA 02139, USA*

<sup>h</sup>*Department of Bio-Analytical Science, University of Science and Technology, Daejeon 34113, Republic of Korea*

**\*To whom correspondence should be addressed.**

\*S. Chung, Tel: +82 2 3290 3352; Email: sidchung@korea.ac.kr.

\*J. A. Kim, Tel: +82 43 240 5068; Fax: +82 43 240 5158; Email: jakim98@kbsi.re.kr.

# Table of contents

<b>Experimental Section</b> .....	2
<b>Results</b> .....	10
<b>Table S1.</b> Molecular coefficients in computer simulation.....	10
<b>Table S2.</b> Real-time qRT-PCR primer paris.....	11
<b>Figure S1.</b> Design of the gel units.....	12
<b>Figure S2.</b> Graphs showing success rate of gel filling affected by plasma treatment.....	13
<b>Figure S3.</b> Comparison of molecular distribution between experiments and simulations..	14
<b>Figure S4.</b> Viability of differentiated ReN cells in the gel unit.....	15
<b>Figure S5.</b> Comparison of biological changes between cells cultured in mono- and co-culture of cells in the gel unit.....	16
<b>Figure S6.</b> HCS image analysis.....	17
<b>References</b> .....	18

## **EXPERIMENTAL SECTION**

### **Fabrication process**

The units that incorporated the hydrogel with a micropillar array for integrating with a micro-well plate were designed using an AutoCAD software (Autodesk, USA). The gel unit in the single well consists of two circular regions in contact with each other, i.e., a circular gel chamber (3-5 mm in diameter) and an inlet hole (1 mm in diameter) and its support for loading the gel. The circular-, elliptical-, and trapezoidal-shaped micropillar features were arrayed around the gel chamber with five different gap distances (200-600  $\mu\text{m}$ ) between micropillars (Fig. S1). The diameter of the horizontal section of the micropillars was 300  $\mu\text{m}$ . A silicon (Si) master mold was fabricated for the gel units using the standard soft lithography process<sup>1</sup> or the gel that was 200  $\mu\text{m}$  deep and deep reactive-ion etching (DRIE) for the gel that was 500  $\mu\text{m}$  deep. After the fabrication was completed, the Sylgard 184 elastomer (polydimethylsiloxane, PDMS, Dow Corning, USA) was poured on a Si master mold with a thickness of about 1 mm and baked at 80 °C for 2 hr for polymerization. After peeling off the PDMS replica, the dumbbell-shaped the gel units were cut out along their outlines using a custom-made punch. The inlet holes also were punched. The plate was completed by bonding of the gel units made of PDMS onto the center of the bottom of the glass of each well in a 24-well plate (MatTek Corporation, USA) or a 96-well plate (Sensoplate™, Greiner Bio-One, Germany) by plasma treatment (100 W, 1 min).

### **Hydrogel filling**

Gel loading tests were performed to verify the stability and reproducibility of the gel used to fill in the culture plate that had been fabricated. 2 mg mL<sup>-1</sup> of collagen solution were used for this test.

2.5-5.5  $\mu\text{L}$  of collagen solution were loaded into the gel units (200  $\mu\text{m}$  deep) with different diameters and gap distances between the micropillars, and different shapes of the micropillars through the inlet hole by pipetting. Three gel units in each dimension were tested, and three random images were taken at each condition and used for analysis. The maximum protrusion length defined by the protruded length of the gel from a circumscribed circle of the micropillars was measured using 9-36 gel units of each dimension. Also, the success and failure rates of the gel filling process were investigated in a time-dependent manner to observe how rapidly the hydrophobic surface was recovered after plasma treatment for use in determining the point in time when the gel should be loaded.

### **Molecular distribution in a gel**

Computational fluid dynamics (CFD) software was used to simulate a dynamic concentration gradient generated in a hydrogel in a platform using a finite element method (FEM) (COMSOL Multi Physics ver.3.4). The simulation used 96- and 24-well format plates, 3 mm and 5 mm in diameter, respectively. Three fluorescein isothiocyanate (FITC)-dextrans varying in size (4, 40, and 70 kDa) were used to simulate transport of growth factors and other molecules.<sup>2</sup> The initial concentration of FITC-dextran in medium was 10  $\mu\text{M}$  and was maintained constant in the medium. Meanwhile, the initial concentration of FITC-dextran in the hydrogel was 0  $\mu\text{M}$ . Diffusion profiles were obtained at 0, 40, 160, 640, and 2,560 min. Simulation for cytokines secreted by cells was performed in a 96-well format plate (3 mm diameter, 200  $\mu\text{m}$  deep). The total cell number in the hydrogel was set for 5,625 cells ( $75 \times 75$ ) by considering hydrogel volume (5.6  $\mu\text{L}$ ), seeding cell density ( $1 \times 10^7$  cells  $\text{mL}^{-1}$ ) and cell-to-cell spacing vertically (20  $\mu\text{m}$ , assumed). IL-1 $\beta$  was chosen

as the secreted model cytokine<sup>3</sup> and each single cell was supposed as having equal reproductive ability. Diffusion profiles were obtained at 0, 60, 240, and 960 min. The diffusion coefficients used in simulation are listed in Table S1. A diffusion test was performed to compare the molecular distribution between the experiments and the simulations. After the gel was solidified, it was immersed completely in the medium, and a single drop of 70 kDa FITC-dextran solution (Sigma-Aldrich, USA) was added carefully to the medium outside the gel unit to maintain a concentration of 10  $\mu\text{M}$ . The concentration gradient of the gel was monitored using a fluorescence microscope (Axio Observer. Z1, Carl Zeiss, Germany), and ImageJ software was used to quantify the intensity of the fluorescence.

### **Cell culture**

An immortalized human neural progenitor cell line (hNPC), ReNcell VM (ReN cell) (Millipore, USA), was cultured in the gel unit-integrated well plate. For proliferation, cells were cultured in a complete growth medium composed of DMEM/F-12 (Gibco, USA), B27 supplement (Gibco, USA), 1% (v/v) penicillin-streptomycin (Sigma-Aldrich, USA), 0.1% of heparin (Sigma-Aldrich, USA), 20 ng mL<sup>-1</sup> of bFGF (Millipore, USA), and 20 ng mL<sup>-1</sup> of EGF (Millipore, USA). To induce differentiation of the ReN cells, the medium was switched to the differentiation medium containing B27 supplement and heparin without bFGF and EGF for an additional 1-2 weeks. For 3D differentiation of the ReN cells, the cells were dissociated with Accutase® (Gibco, USA) and counted using a disposable haemocytometer (C-chip, INCYTO, Korea) to adjust the final cell concentration to about  $7 \times 10^6 - 1 \times 10^7$  cells mL<sup>-1</sup> in the final 5 mg mL<sup>-1</sup> of Matrigel solution. The gel solution containing the cells was loaded into the gel units in the well and incubated at 37 °C

for 30 min for solidification. During the differentiation of the cells, the medium was freshly changed every three days. The previously engineered ReN cells overexpressing genes with familial AD (FAD) mutations produced a high concentration of pathogenic amyloid  $\beta$  ( $A\beta$ ) species, which also were cultured and differentiated as an Alzheimer's disease model.<sup>4,5</sup> Human dermal microvascular endothelial cells, i.e., HMVEC-D (Lonza, USA), were cultured with the EGM-2MV BulletKit medium (Lonza, USA) for co-culture. After detachment, the cells were diluted to a final concentration of  $2 \times 10^5$  cells  $mL^{-1}$  in the medium. For co-culture, ReN cells were three-dimensionally differentiated in the gel unit for a week and then the HMVEC-D cells were seeded into the outer region of the gel unit in the same well. The media for co-culture were supplied with a 1:1 mixture of EGM-2MV and differentiation media of ReN cells.

### **Viability and cytotoxicity test**

To investigate the viability of the ReN cells cultured and differentiated in the gel unit (5 mm in diameter), a cell viability test was performed using a LIVE/DEAD<sup>TM</sup> viability kit (Thermo Fisher Scientific, USA). Three week-differentiated cells were incubated for 90 min in DPBS (Gibco) with 4  $\mu$ M calcein-AM and 2  $\mu$ M ethidium homodimer-1 at 37 °C in a 5% CO<sub>2</sub> incubator. After staining, the devices were rinsed twice with DPBS, and images were acquired using a fluorescence microscope. The viability of the ReN cells cultured in the gel units in a cell density-dependent manner were determined in a 96-well format plate (3 mm diameter, 200  $\mu$ m deep), and then ATP signals released from the cells were measured using a CellTiter-Glo<sup>®</sup> 3D cell viability assay kit (Promega, USA) according to the manufacturer's directions. The 2  $\times$  luciferase-based reagent in a kit was added to the 3D cells in the well and shaken for 50 minutes for lysis. The luminescence

intensity was measured directly using a microplate reader (SpectraMax L, Molecular Devices, USA). For the cytotoxicity test, the 1-week differentiated ReN cells were incubated with dimethyl sulfoxide (DMSO, Sigma-Aldrich, USA) for 24 hr in a dose-dependent manner (0.1- 20% (v/v)). The cytotoxicity levels of the cells were measured in the same manner and plotted against the DMSO concentration.

### **Quantitative real-time PCR**

ReN cells were differentiated for a week in the gel unit in a 24-well format plate (5 mm diameter, 500  $\mu$ m deep); then total RNAs were collected and purified with a RNeasy<sup>®</sup> mini kit (QIAGEN, Germany). The RNA yields were measured using a nanophotometer<sup>™</sup> (P330, IMPLEN, Germany). Total RNAs of 20 ng were reverse-transcribed using a ReverTra Ace<sup>®</sup> qPCR RT Master Mix with a gDNA Remover kit (Toyobo Co., Japan), and 2  $\mu$ l of cDNAs were mixed with a qPCR master mix (Power SYBR<sup>®</sup> Green PCR Master Mix, Applied Biosystems, USA). The 40 amplification cycles of the samples were performed by a real-time PCR thermal cycler (QuantStudio 3, Applied Biosystems, USA). The primers and their sequences used for qRT-PCR are listed in Table S2.<sup>6</sup> To investigate the differentiation level into neuron and glia, MAP2 and GFAP were examined, and GAPDH was used as an internal control.

### **Immunocytochemistry and Western blot analysis**

ReN cells mixed in Matrigel solution were loaded into gel units (5 mm diameter, 500  $\mu$ m deep) in a 24-well format plate and differentiated for 2 weeks. After fixation with 4% (v/v) paraformaldehyde for 20 min at room temperature (RT), the cells were permeabilized with 0.1%

(v/v) Triton X-100 in DPBS for 20 min. After rinsing, cells were blocked with 3% (w/v) bovine serum albumin (BSA, MP Biomedicals, France) for 1 hr at RT in DBPS containing 0.1% (v/v) Triton X-100. To observe the level of cell differentiation, a neuronal marker, MAP2, and a glial marker, GFAP were examined. The anti-MAP2 (1:100, Cell Signaling, USA) and anti-GFAP (1:300, Cell signaling, USA) antibodies were used as the primary antibodies. The primary antibodies were diluted with 1% (w/v) BSA solution that contained 0.1% (v/v) Tween-20 (Duchefa Biochemie, Netherlands) in DBPS. Alexa Fluor® 488- and 594-conjugated secondary antibodies (1:1000, Invitrogen, USA) diluted in 1% (w/v) BSA solution containing 0.1 % (v/v) Tween-20 in DPBS were used and the nuclei were stained with Hoechst 33342 (Thermo Fisher Scientific, USA). Fluorescence images were taken using a fluorescence microscope.

For Western blot analysis, 1-week differentiated ReN cells in the gel-units (5 mm diameter, 500 µm deep) were lysed using RIPA buffer (Thermo Fisher Scientific, USA) for 20 mins at 4 °C in the presence of a protease inhibitor cocktail (Roche, Germany). The cell lysates were centrifuged for 15 mins at 12,000 rpm, and the concentration of the protein obtained from the supernatant was estimated using a BCA assay kit (Thermo Fisher Scientific, USA). 20 µg of protein were loaded in each well of Bolt™ 4-12% Bis-Tris Plus Gel (Invitrogen™, USA) and electro-transferred to a PVDF membrane (GE Healthcare, USA). The membrane was rinsed with tris-buffered saline buffer containing 0.2% (v/v) Tween-20 (TBST), blocked in TBST with 5% (w/v) skim milk (Difco, USA) for 1 hr at RT, and then it was incubated overnight at 4 °C in primary antibody solutions (1:1000 MAP2, 1:1000 GFAP, 1:500 GAPDH) diluted in TBST with 1% (w/v) skim milk. The membrane was rinsed with TBST and incubated with secondary antibody (1:2000) diluted in TBST for 1 hr at RT. The membrane was washed with TBST and then the reacted

chemiluminescent signals by ECL solution (GE Healthcare, USA) were detected using a gel imaging system (ImageQuant 350, GE Healthcare, USA).

### **Neural differentiation analysis using high content screening (HCS)**

ReN cells were differentiated for 2 weeks in the gel units in a 96-well format plate with chemical compounds promoting (Mevastatin, Sigma-Aldrich, USA) or suppressing (2-Chloroadenosine, Sigma-Aldrich, USA) the level of neuronal differentiation,<sup>7</sup> and the control cells were treated with the same amount of DMSO (0.05% (v/v)). Half of the medium was refreshed every three days with the compound level maintained at 5  $\mu$ M. The cells were fixed and immunostained with anti-MAP2 primary antibody and Alexa 488-tagged secondary antibody to determine the neurogenesis level. The fluorescence images that were acquired on the 96-well plate using a high-content imaging system (Operetta CLS™, PerkinElmer, USA) were quantified using image analysis software (Harmony ver. 4.6, PerkinElmer, USA) to determine the enhanced or suppressed levels of neuronal differentiation compared to the control cells.

### **ELISA assay**

As a proof of concept for drug screening using the developed plate, drug efficacy tests were performed with an AD model cell line, FAD-ReN cell, differentiated in the 24-well format plate. After 2 weeks of differentiation, the cells were treated with inhibitors of A $\beta$  production, such as 1  $\mu$ M  $\beta$ -secretase inhibitor IV (BACE 1 inhibitor, Merck, USA), 1  $\mu$ M DAPT (Merck, USA), and 3.7 nM, Compound E (Merck, USA). The cells treated with DMSO (0.01%) were used as the control. Half of the medium was refreshed every three days with the inhibitors. After 1 week of

treatment with the inhibitors, the change in the levels of A $\beta$ 40 and A $\beta$ 42 levels secreted into the conditioned media were quantified using a human A $\beta$  ELISA assay kit (Wako, Japan), and the absorbance signal was measured using a microplate reader (DTX 880, Beckman Coulter, USA).

### **Statistical analysis**

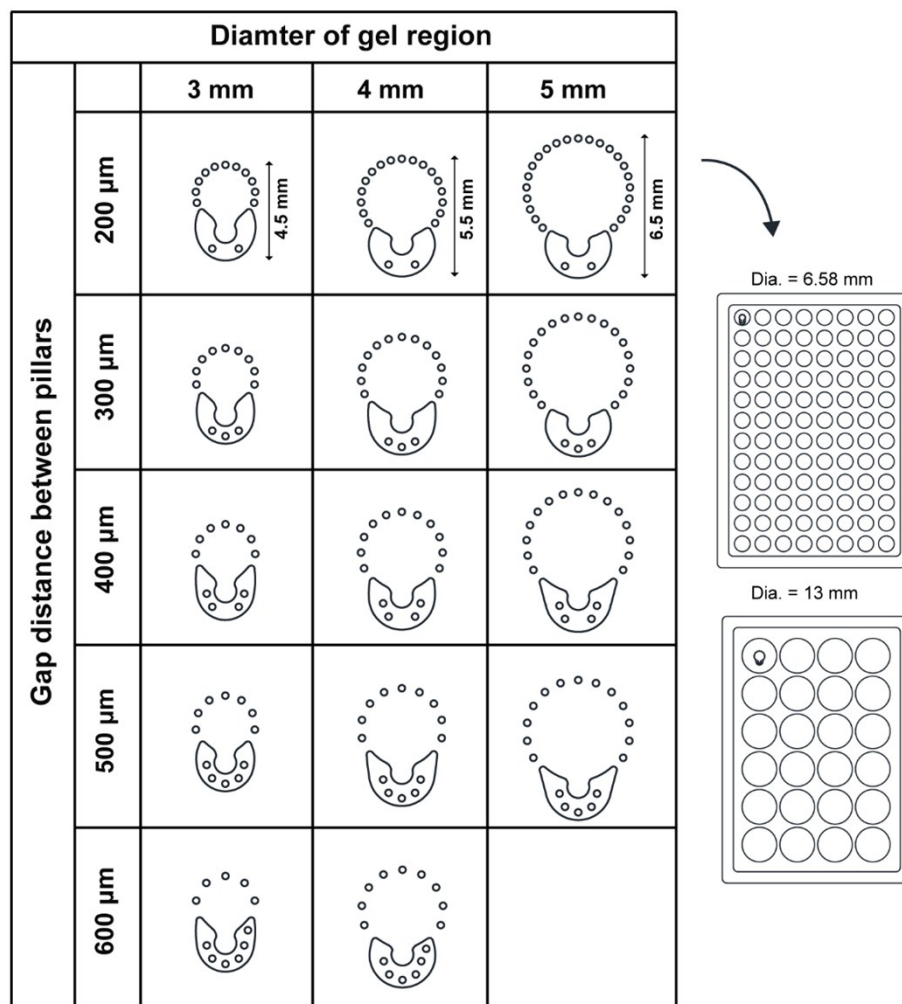
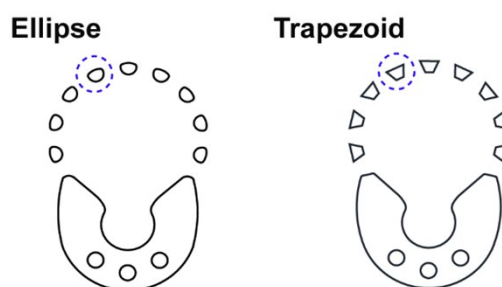
For quantitative analysis, all of the experiments were performed with a minimum of three-replicate samples at each condition. The statistical analyses were carried out using a two-tailed Student's *t*-test. The data presented in the graphs are the average values, and the error bars represents the standard deviation (S.D.). Image analysis was performed with the representative images acquired by the fluorescence microscope, and the maximum projection images of replicate samples acquired by the HCS image system were analyzed using the HCS image software (Harmony ver. 4.6, PerkinElmer, USA). The asterisks indicate the respective values of the statistically significant differences, i.e., \*,  $p < 0.05$ ; \*\*,  $p < 0.01$ ; \*\*\*,  $p < 0.001$ .

**Table S1.** Molecular coefficients in computer simulation<sup>2,3</sup>

<b>Molecular type</b>	<b>Diffusion coefficient in medium (m s<sup>-1</sup>)</b>	<b>Diffusion coefficient in hydrogel (m s<sup>-1</sup>)</b>	<b>Secretion rate (nM min<sup>-1</sup> cell<sup>-1</sup>)</b>
4 kDa FITC-dextran	1.35 x 10 <sup>-10</sup>	1.27 x 10 <sup>-10</sup>	N/A
40 kDa FITC-dextran	4.50 x 10 <sup>-11</sup>	4.23 x 10 <sup>-11</sup>	N/A
70 kDa FITC-dextran	2.30 x 10 <sup>-11</sup>	2.16 x 10 <sup>-11</sup>	N/A
IL-1 $\beta$	3.00 x 10 <sup>-11</sup>	2.82 x 10 <sup>-11</sup>	0.366

**Table S2.** Real-time qRT-PCR primer pairs<sup>6</sup>

<b>Gene name</b>	<b>Forward primer sequences</b>	<b>Reverse primer sequences</b>	<b>Product size (bp)</b>	<b>Gene Bank Accession</b>
GAPDH	GTCAGTGGTGGACCTG ACCT	CACCACCCTGTTGCTG TAGC	256	NM_001256799
MAP2	CGCTCAGACACCCTTCA GATAAC	AAATCATCCTCGATGG TCACAAC	122	NM_002374
GFAP	CAACCTGCAGATTCGAG AAA	GTCCTGCCTCACATCA CATC	153	NM_002055

**A****B**

**Figure S1.** (A) Designs of the gel units with different diameter chambers (3-5 mm) and gap distances (200-600  $\mu\text{m}$ ) between micropillars for integration with multi-well plates (24-well plate or 96-well plate). (B) Additional cross-sectional shapes of the micropillars; elliptical and trapezoidal shapes.

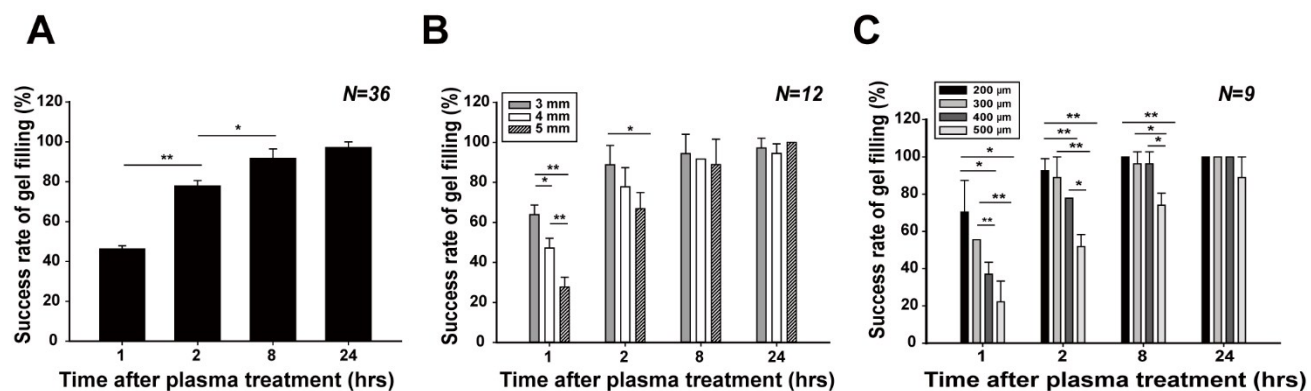


**Figure S2.** (A) Success rate of gel filling according to the time after plasma treatment on the surface of PDMS. The success rate of gel filling according to the time after plasma treatment by varying (B) the gel diameters; (C) the gap distances between micropillars. \* $p < 0.05$ , \*\* $p < 0.01$ .

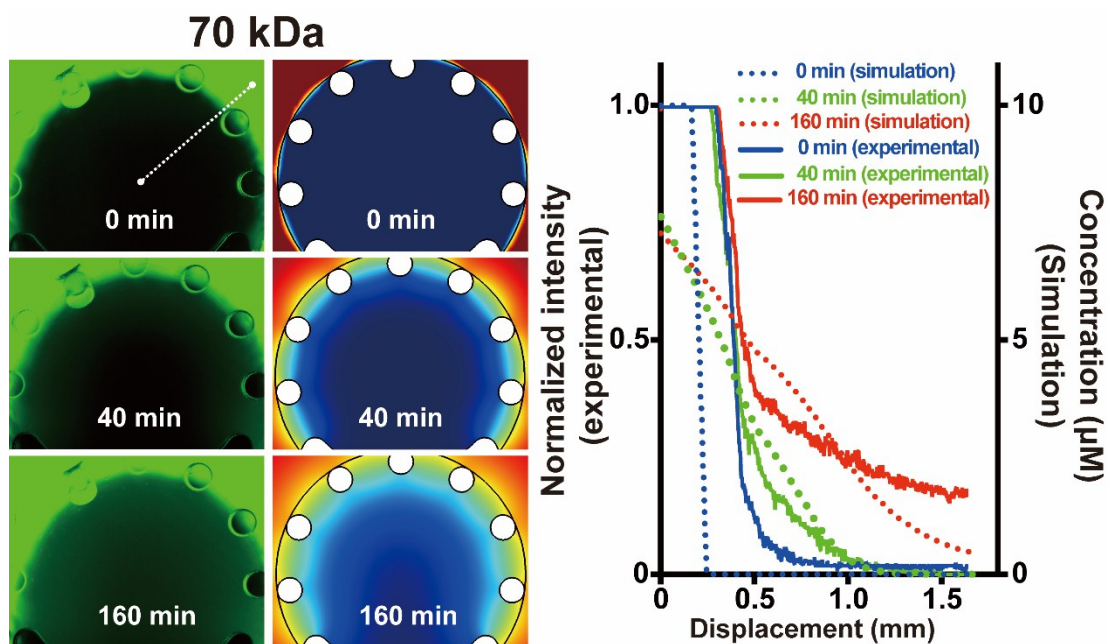


**Figure S3.** Comparison of the molecular distribution in a hydrogel between the experimental and simulation data. A 70 kDa FITC-dextran was tested in the gel unit with a diameter of 3 mm. The intensity of fluorescence of the gel with a concentration gradient was analyzed using the ImageJ program.

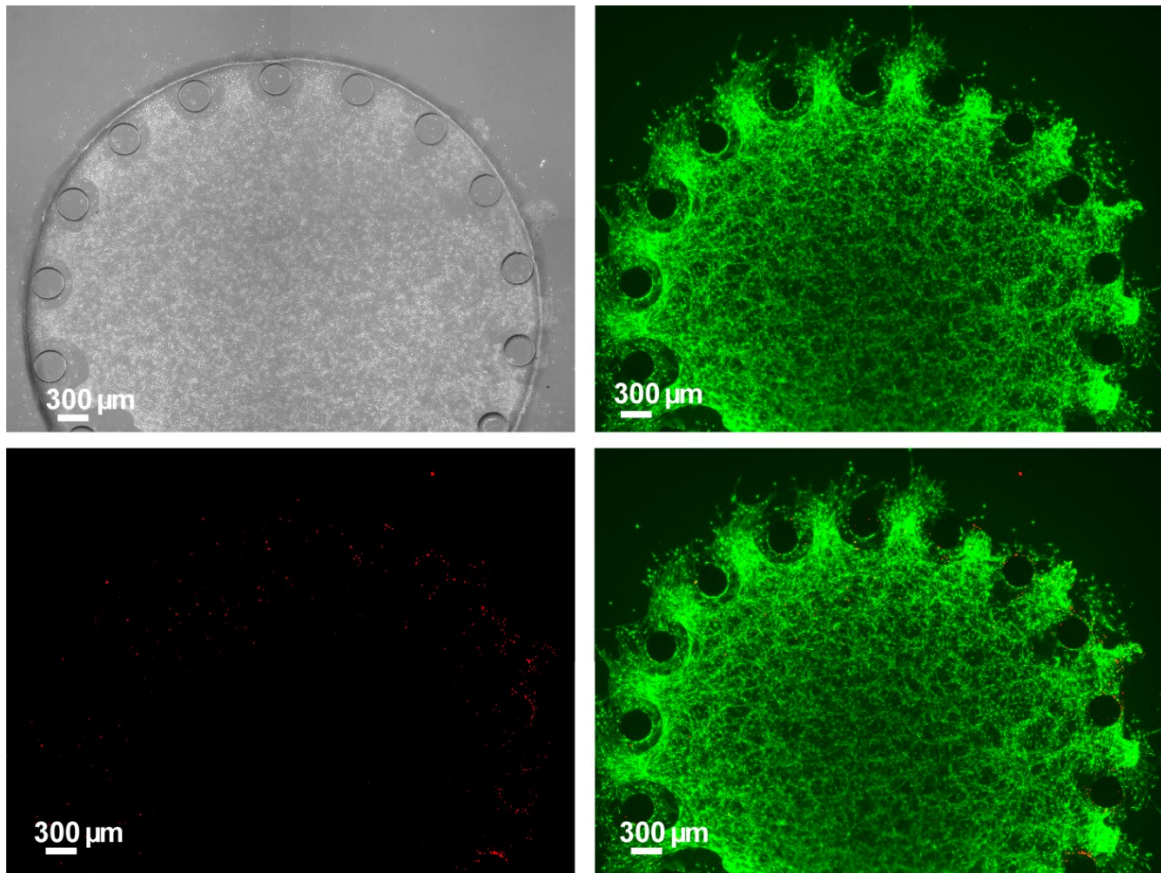


**Figure S4.** Viability of ReN cells after 3 week-differentiation. The cells were differentiated for two weeks and then exposed to 0.01% DMSO for another one week. The cells were stained for viability (4  $\mu\text{M}$  calcein AM/ 2  $\mu\text{M}$  ethidium homodimer-1) using a LIVE/DEAD™ cell viability assay kit. The diameter of the gel units was 5 mm.

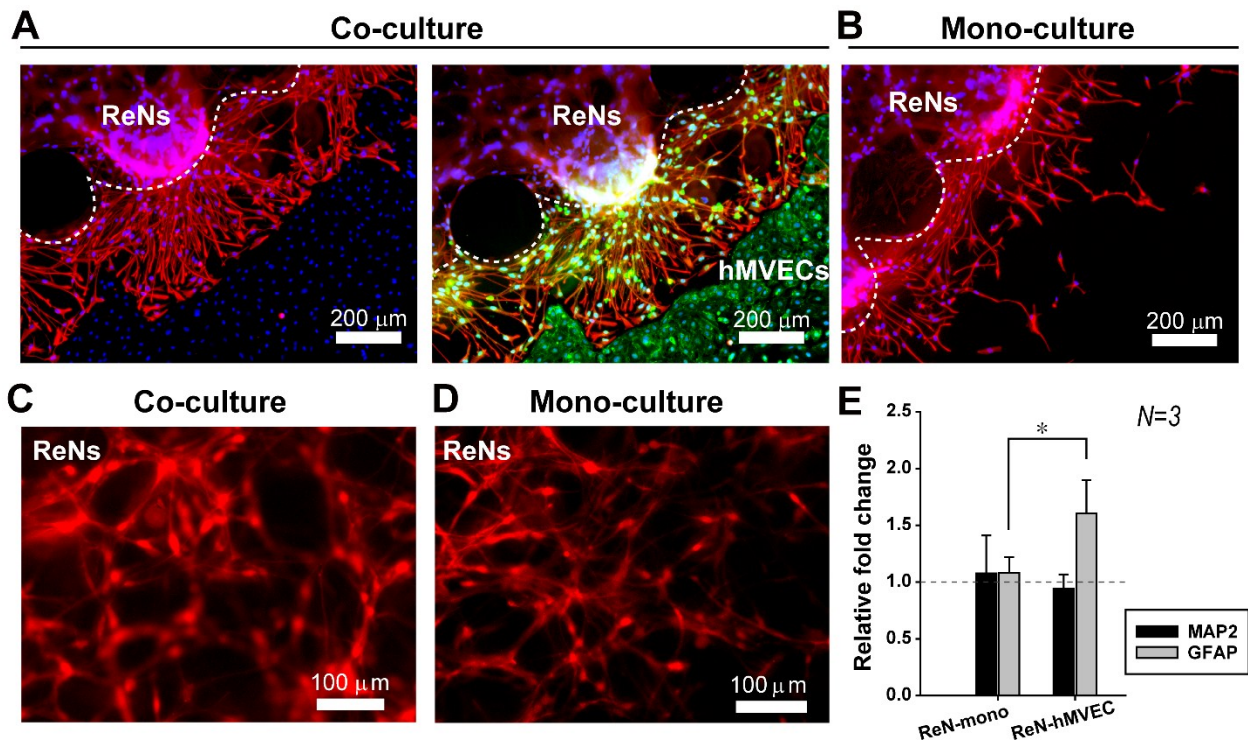


**Figure S5.** Comparison between ReN and hMVEC mono-culture and ReN-hMVEC co-culture in the gel units. The ReN cells were differentiated for a week, and hMVECs were co-cultured for 4 days on the space adjacent to the gel unit in the same well. Representative images of the (A) ReN-hMVEC co-culture (B) ReN mono-culture, (C) ReNs in co-culture, and (D) ReNs in mono-culture. Cells were immunostained against nuclei (blue), VE-cadherin (ECs, green), and GFAP (Glial, red). (E) qRT-PCR analysis of the GFAP and MAP2 normalized to GAPDH from the cells in the mono- and co-culture.  $*p < 0.05$ , in comparison with ReN-mono culture.

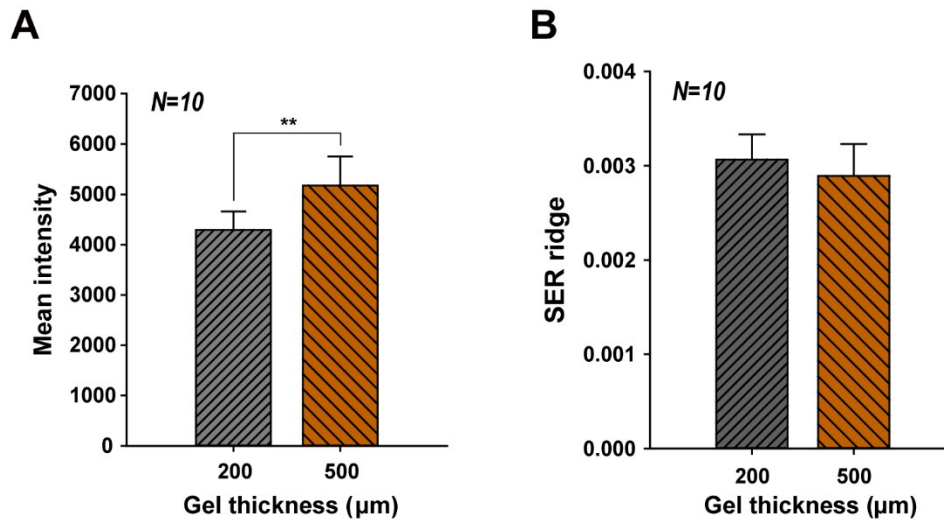


**Figure S6.** Analysis of the high content screening (HCS) images in 3D differentiated ReN cells expressing mCherry in two different thick-gels (200 μm and 500 μm). The z-sliced images (1 μm-step size) in the middle of the gels from 10 replicate samples were obtained and processed by maximum projection (total 100 μm deep). The cells in the center of the gel unit were observed in each well using the 20 × objective lens (9 fields, 645 μm × 645 μm/ field). Quantitative image analysis was conducted using the Harmony software for investigating (A) the mean intensity and (B) the SER ridge of the acquired images, with  $**p < 0.01$ , between the two different thick-gels.

## References

1. J. A. Kim, J. Y. Lee, S. Seong, S. H. Cha, S. H. Lee, J. J. Kim and T. H. Park, *Biochem. Eng. J.*, 2006, **29**, 91-97.
2. T. Kihara, J. Ito and J. Miyake, *PLoS One*, 2013, **8**, e82382.
3. G. J. Goodhill, *Eur. J. Neurosci.*, 1997, **9**, 1414-1421.
4. Y. H. Kim, S. H. Choi, C. D'Avanzo, M. Hebisch, C. Sliwinski, E. Bylykbashi, K. J. Washicosky, J. B. Klee, O. Brüstle and R. E. Tanzi, *Nat. Protoc.*, 2015, **10**, 985-1006.
5. S. H. Choi, Y. H. Kim, M. Hebisch, C. Sliwinski, S. Lee, C. D'Avanzo, H. Chen, B. Hooli, C. Asselin and J. Muffat, *Nature*, 2014, **515**, 274-278.
6. J. Park, N. Lee, E. K. Choe, M. K. Kim, J. Lee, M. S. Byun, M.-W. Chon, S. W. Chon, S. W. Kim, J. C. Lee, *Sci. Rep.* 2017, **7**, 10166.
7. J. H. Rhim, X. Luo, X. Xu, D. Gao, T. Zhou, F. Li, L. Qin, P. Wang, X. Xia and S. T. Wong, *Sci. Rep.*, 2015, **5**, 16237.